



Since January 2020 Elsevier has created a COVID-19 resource centre with free information in English and Mandarin on the novel coronavirus COVID-19. The COVID-19 resource centre is hosted on Elsevier Connect, the company's public news and information website.

Elsevier hereby grants permission to make all its COVID-19-related research that is available on the COVID-19 resource centre - including this research content - immediately available in PubMed Central and other publicly funded repositories, such as the WHO COVID database with rights for unrestricted research re-use and analyses in any form or by any means with acknowledgement of the original source. These permissions are granted for free by Elsevier for as long as the COVID-19 resource centre remains active.



A SARS-CoV-2 vaccine based on conjugation of SARS-CoV-2 RBD with IC28 peptide and mannan

Yunxia He^{a,b,1}, Weili Yu^{a,1}, Lijuan Shen^a, Wenying Yan^{a,b}, Lucheng Xiao^{a,b}, Jinming Qi^{a,*}, Tao Hu^{a,*}

^a State Key Laboratory of Biochemical Engineering, Institute of Process Engineering, Chinese Academy of Sciences, Beijing 100190, China

^b University of Chinese Academy of Sciences, Beijing 100190, China

ARTICLE INFO

Keywords:
SARS-CoV-2
RBD
Adjuvant

ABSTRACT

SARS-CoV-2 is a particularly transmissible virus that causes a severe respiratory disease known as COVID-19. Safe and effective vaccines are urgently needed to combat the COVID-19 pandemic. The receptor-binding domain (RBD) of SARS-CoV-2 spike protein elicits most neutralizing antibodies during viral infection and is an ideal antigen for vaccine development. In particular, RBD expressed by *E. coli* is amenable to low cost and high-yield manufacturability. The adjuvant is necessitated to improve the immunogenicity of RBD. IC28, a TLR5-dependent adjuvant, is a peptide from bacterial flagellin. Mannan is a ligand of TLR-4 or TLR-2 and a polysaccharide adjuvant. Here, IC28 and mannan were both covalently conjugated with RBD from *E. coli*. The conjugate (RBD-IC28-M) elicited high RBD-specific IgG titers, and a neutralization antibody titer of 201.4. It induced high levels of Th1-type cytokines (IFN- γ) and Th2-type cytokines (IL-5 and IL-10), along with high antigenicity and no apparent toxicity to the organs. The mouse sera of the RBD-IC28-M group competitively interfered with the interaction of RBD and ACE2. Thus, conjugation with IC28 and mannan additively enhanced the humoral and cellular immunity. Our study was expected to provide the feasibility to develop an affordable, easily scalable, effective vaccine SARS-CoV-2 vaccine.

1. Introduction

SARS-CoV-2, a β -coronavirus in the coronavirus family, is a particularly transmissible virus that causes the worldwide viral pandemic and a severe respiratory disease known as COVID-19 [1]. COVID-19 is characterized by a respiratory syndrome with a variable degree of severity, ranging from a mild upper respiratory tract illness to severe interstitial pneumonia and acute respiratory distress syndrome (ARDS) [2]. The COVID-19 pandemic is a major ongoing challenge to global public health affecting 216 countries or regions [3]. As of September 8, 2022, there have been a total of 603,711,760 reported SARS-CoV-2 infections and 6,484,136 related deaths around the world [4]. The recent emergence of several SARS-CoV-2 variants and variants of concern (VOCs) is especially worrisome, including B.1.1.7 (alpha), B.1.351 (beta), B.1.427/B.1.429 (epsilon), P.1 (gamma), B.1.617.2 (delta) and B.1.1.529 (Omicron) [5–7]. Thus, the development of safe and effective vaccine strategy is urgently needed to combat the SARS-CoV-2 infection

[8].

Recently, various SARS-CoV-2 vaccines have been developed [9,10], based on the inactivated viruses [11], recombinant viral vectors [12,13], DNA [14] or mRNA [15], and recombinant proteins [16]. These vaccines have shown high efficacy in preclinical and clinical studies [17,18]. High vaccine effectiveness (VE) of these vaccines against SARS-CoV-2 was observed through clinical trials, such as 70.4 % VE of the ChAdOx1 vaccine (AZD1222; Oxford-AstraZeneca), 95 % VE of the BNT162b2 mRNA vaccine (Pfizer-BioNTech), 94.1 % VE of the mRNA-1273 vaccine (Moderna), and 50.7 % VE of an inactivated COVID-19 vaccine (CoronaVac) [19,20]. However, worldwide access to these vaccines was limited by the high cost, and concerns regarding global production capacity and scalability especially in low and middle-income countries [21].

Importantly, the vaccine based on recombinant proteins receives much attention for their specificity, effectiveness, and safety [22]. For example, NVX-CoV2373 (Novavax Inc.) was a protein-based COVID-19

* Corresponding authors.

E-mail addresses: qjinming@home.ipe.ac.cn (J. Qi), thu@home.ipe.ac.cn (T. Hu).

¹ The authors contribute equally to the work.

vaccine using Novavax's proprietary nanoparticle technology. It showed high immunogenicity and safety, along with stimulating high levels of neutralizing antibodies in clinical studies [23]. As a structural protein of SARS-CoV-2, spike glycoprotein is capable of binding to hACE2 and initiating membrane fusion and virus entry, which can bind to a host receptor, angiotensin converting enzyme 2 (ACE2) through the receptor-binding domain (RBD) [24,25]. RBD of SARS-CoV-2 spike protein elicits most neutralizing antibodies during viral infection [26]. Blocking the interaction of RBD with hACE2 was a strategy for the design of antiviral agents, and RBD was thus a potential target antigen for vaccine development [27]. However, the low immunogenicity of RBD limits its vaccine development, due to the absence of pathogen-associated molecular patterns to activate the immune system [28].

The glycan moieties of RBD have a relevant role in the stability and immunogenicity of RBD [29]. RBD has been expressed in the eukaryotic cell expression systems (e.g., HEK293 cells), which suffers from low expression yield and high cost [30,31]. SARS-CoV-2 RBD expressed by *E. coli* is a cost-effective antigen without the glycan moieties, which has been used for serological testing [32]. RBD expressed by *E. coli* exhibited a weaker interaction with ACE2 than that expressed by HEK293 cells with glycosylation [33]. In order to develop worldwide accessible and scalable vaccines for low and middle-income countries, the affordable and easily scalable RBD expressed by *E. coli* was the ideal antigen. Recently, RBD was produced in *E. coli* when fused to a fragment of CRM₁₉₇. The CRM₁₉₇-RBD chimera exhibited the competence in binding ACE2 and a high stability at room temperature, which may be developed a candidate vaccine against COVID-19 [34].

Structural biology-based vaccine design has been employed to enhance the immune effectiveness of RBD, such as recombinant tandem-repeat dimeric RBD [35]. Alternatively, appropriate adjuvants and the delivery system are complementary to increase the immunogenicity of vaccine antigens by activating the pattern-recognition receptors or by modulating antigen pharmacokinetics [36,37]. Alum salts, LPS, MF59 and AS04 have been approved as adjuvants vaccine for clinical use [38,39]. However, these adjuvants may result in several adverse effects such as inflammation, toxicity, allergy, and immunosuppression [37].

Toll-like receptor agonists have received much attention for their high adjuvant activity. Bacterial flagellin activates the innate immune system and ultimately the adaptive immune system through a Toll-like receptor 5 (TLR5)-dependent signaling mechanism [40]. The peptide from bacterial flagellin (IC28) with deletions of D2 and the distal part of D1 of FliC_{Δ174–400} was considered as a TLR5-dependent adjuvant for vaccination [41]. IC28 does not impact on antigenicity and does not significantly modify the immunostimulatory adjuvant activity of flagellin [42]. Mannan is a biocompatible polysaccharide from yeast, and a ligand of TLR-4 or TLR-2. Mannan is an adjuvant that can stimulate cellular and humoral immunity [43–45]. Interestingly, the mixture of several adjuvants with different immunomodulatory mechanisms showed the additive adjuvant effect to increase the immunogenicity of an antigen [46].

In the present study, RBD expressed by *E. coli* was covalently conjugated with IC28 and mannan to improve the immunogenicity of RBD. Conjugation ensured the simultaneous capture of the two adjuvants and RBD by the antigen presenting cells (APCs), which in turn elicited a strong immune response. The conjugate (RBD-IC28-M) was structurally characterized. The antigenicity and immunogenicity of RBD-IC28-M were evaluated in the BALB/c mice. The potential toxicity of RBD-IC28-M were evaluated. Thus, RBD-IC28-M was expected to act as an affordable, easily scalable and effective SARS-CoV-2 vaccine.

2. Materials and methods

2.1. Materials

IC28 peptide with a cysteine residue at the C-terminus was synthesized by GL Biochem Co. (Shanghai, China). Human angiotensin-

converting enzyme 2 (hACE2), hACE2-specific rabbit antibody, and HRP-conjugated goat antirabbit IgG antibody were ordered from Sino Biological (Beijing, China). Mannan from *S. cerevisiae*, 1-anilino-8-naphthalene sulfonic acid (ANS), 6-maleimidohexanoic acid *N*-hydroxysuccinimide ester (EMCS), sodium cyanoborohydride, dithio-bis-(2-nitrobenzoic acid (DTNB) and 3,3',5,5'-tetramethylbenzidine (TMB) were purchased from Sigma (USA). Horse radish peroxidase (HRP)-conjugated goat anti-mouse IgG Fc antibody (HRP-IgG), IgG1 Fc antibody (HRP-IgG1), IgG2a Fc antibody (HRP-IgG2a) and IgM Fc antibody (HRP-IgM) were purchased from Abcam (USA). IFN- γ ELISA kit was ordered from Biolegend (USA). IL-5 and IL-10 ELISA kits were purchased from Invitrogen (USA).

2.2. Expression and purification of RBD

The coding DNA sequence of RBD of SARS-CoV-2 S protein (amino acid 330–583 of S protein) was from strain Wuhan-Hu-1 (Genbank Acc. No. 045512.2). RBD was expressed in *E. coli* and purified from the renaturation solution by a Ni Sepharose Fast Flow column (0.5 cm \times 5 cm, GE Healthcare, USA) as previously described [33].

2.3. Preparation of the conjugates

2.3.1. Preparation of RBD-IC28

RBD (0.6 mg) was incubated with 10-fold molar excess of EMCS in 20 mM PB buffer (pH 7.4) at 4 °C for overnight (Fig. 1). The free EMCS was removed by extensive dialysis of the reaction mixture against 20 mM PB buffer (pH 7.4). The EMCS-modified RBD (0.6 mg) was mixed with IC28 (0.1 mg) in 20 mM PB buffer (pH 7.4) to obtain the RBD-IC28 conjugate (RBD-IC28) at 4 °C for overnight (Fig. 1). The incubation at 4 °C could avoid the denaturation of RBD during the incubation period.

2.3.2. Preparation of RBD-M

Mannan (10 mg/mL, 1 mL) was oxidized by addition of 0.1 M NaIO₄ (0.2 mL) in 20 mM sodium acetate buffer (pH 5.6). The reaction was kept in the dark for 40 min at room temperature, followed by extensive dialysis of the reaction mixture against 20 mM PB buffer (pH 7.4). RBD (0.6 mg) was then mixed with the oxidized mannan (3 mg) and sodium cyanoborohydride (3 mg) in 20 mM PB buffer (pH 7.4). The mixture was incubated at 4 °C for overnight to obtain the conjugate (RBD-M) (Fig. 1).

2.3.3. Preparation of RBD-IC28-M

The oxidized mannan (2 mg), RBD-IC28 (0.6 mg) and NaBH₃CN (2 mg) were mixed in 20 mM PB buffer (pH 7.4). The mixture was incubated at 4 °C for overnight to obtain the conjugate (RBD-IC28-M) (Fig. 1).

2.4. Purification of the conjugates

A semi-preparative Superdex 200 column (2.6 cm \times 60 cm, GE Healthcare, USA) based on size exclusion chromatography (SEC) was utilized to purify RBD-IC28, RBD-M and RBD-IC28-M. The reaction mixtures containing the three conjugates were loaded on the column and eluted by PBS buffer (pH 7.4) at a flow rate of 2.0 mL/min. The fractions corresponding to the three conjugates were pooled, respectively.

2.5. SDS-PAGE analysis

The three conjugates were analyzed by SDS-PAGE, using a 12 % polyacrylamide gel under a reducing (5 % v/v β -mercaptoethanol) condition. The gel was stained with Coomassie blue R-250.

2.6. SEC analysis

The three conjugates were analyzed by an analytical Sepharose 6

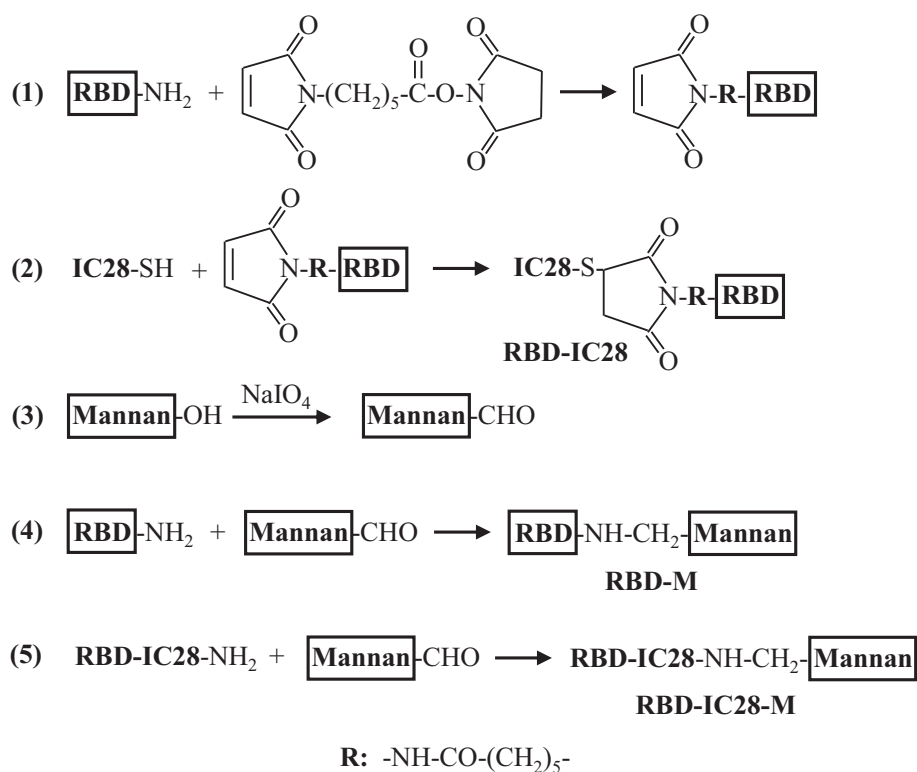


Fig. 1. The scheme for preparation of the conjugates.

column (1 cm × 30 cm, GE Healthcare, USA). The column was equilibrated and eluted with PBS buffer (pH 7.4) at a flow rate of 0.5 mL/min. The effluent was detected at 280 nm.

2.7. Quantitative assay

The RBD contents of the three conjugates were measured by the Bradford method. The IC28 contents of RBD-IC28 and RBD-IC28-M were measured by the DTNB method. The mannan contents of RBD-M and RBD-IC28-M were measured by the phenol-sulfuric acid method, using mannan as the standard.

2.8. Fluorescence spectroscopy

2.8.1. Intrinsic fluorescence spectroscopy

Intrinsic fluorescence measurements of the three conjugates were carried out on a Hitachi F-4500 fluorescence spectropolarimeter (Hitachi, Japan) at room temperature, using a cuvette with 1.0 cm path length. The intrinsic emission spectra were recorded from 300 nm to 400 nm and excited at 280 nm. Excitation and emission slit widths were 5 nm and 10 nm, respectively. The three conjugates were all at a protein concentration of 0.1 mg/mL in 20 mM PB buffer (pH 7.4).

2.8.2. Extrinsic fluorescence spectroscopy

ANS was mixed with the conjugates at a molar ratio of 10:1. The mixtures were measured by extrinsic fluorescence spectroscopy. The emission spectra were recorded from 400 nm to 600 nm and excited at 350 nm. Excitation and emission slit widths were 10 nm and 20 nm, respectively. The three conjugates were all at a protein concentration of 0.1 mg/mL in 20 mM PB buffer (pH 7.4).

2.9. Circular dichroism spectroscopy

Far-UV circular dichroism (CD) spectra of the three conjugates were recorded on a Jasco-810 spectropolarimeter (Jasco, Japan) between

260 nm and 190 nm. A cuvette with a 0.1 cm path length was used. The three conjugates were at a protein concentration of 0.2 mg/mL in 20 mM PB buffer (pH 7.4). The secondary structures were calculated by the structure fitting software that has been built-in to the instrument.

2.10. Immunization

Thirty female BALB/c mice aged at 5 weeks (15–20 g) were randomly divided into five groups for six animals each. All the procedures of the animal experiments have been approved by the Animal Ethical Experimentation Committee of Institute of Process Engineering, Chinese Academy of Sciences (Beijing, China), according to the requirements of the National Act on the Use of Experimental Animals (China). The groups were PBS, RBD, RBD-IC28, RBD-M and RBD-IC28-M groups, which were defined according to the samples immunized. All the samples were at a protein concentration of 0.2 mg/mL in PBS buffer (pH 7.4) except for the PBS group. The mice were immunized with 0.1 mL of the samples by intramuscular injection on days 0, 7, and 14. Blood samples were collected on days 7, 14, and 21. The mice sera was isolated and stored at -80°C until use.

2.11. ELISA assay

The RBD-specific antibodies IgG, IgG1, IgG2a and IgM titers were measured by ELISA. The 96-well plates were pre-coated with RBD (0.75 $\mu\text{g}/\text{well}$) in 50 mM NaHCO_3 (pH 9.6) at 4°C overnight. The plates were blocked with 200 μL of 4 % skimmed milk in PBS buffer (PBS-milk, pH 7.4) at 37°C for 1 h, followed by washing 3 times with PBS buffer (pH 7.4). The diluted sera (100 μL) were added and incubated in the wells for 1 h at 37°C , followed by washing with PBS buffer containing 0.1 % Tween 20 (PBST, pH 7.4). The plates were added with 100 μL of the diluted HRP-IgG, HRP-IgG1, HRP-IgG2a or HRP-IgM at 37°C for 1 h, respectively. After washing 3 times with PBST, 100 μL of 0.015 % (w/v) TMB was added and incubated at 37°C for 30 min, followed by adding 25 μL of 2 M H_2SO_4 . The resultant solution was determined at 450 nm.

The antibody titers were presented as the highest sample dilution, which led to in an OD value >2.1 times the OD mean of the sera of the PBS group.

2.12. Avidity of antibody

The avidity of RBD-specific IgG was determined by the ammonium thiocyanate elution method [47]. Briefly, the plates were pre-coated with RBD (0.75 µg/well). The conjugates were blocked with 200 µL PBS-milk and washed 3 times with PBS buffer (pH 7.4), followed by incubation of the diluted mice sera at 37 °C for 1 h. Afterwards, each plate was incubated with 50 µL of ammonium thiocyanate (0–3.5 M) at 37 °C for 1 h. After a washing cycle, the measurement was repeated. The avidity index (AI) was expressed as ammonium thiocyanate concentration needed to decrease the absorbance by 50 %.

2.13. Antigenicity of the conjugates

The binding affinity of RBD to the receptor hACE2 was assayed by ELISA to evaluate the antigenicity of the conjugates. The 96-well plate was coated with RBD, RBD-IC28, RBD-M and RBD-IC28-M at a protein concentration of 5 µg/mL, respectively. The plate was then incubated with hACE2 that were five-fold serially diluted starting at 10 µg/mL. After washing with PBST, 100 µL hACE2-specific rabbit antibody with 5000-fold dilution was added to each well, followed by incubation at 37 °C for 1 h. After washing with PBST, HRP-conjugated goat anti-rabbit IgG antibody with 10,000-fold dilution was added and incubated for 45 min at 37 °C. Finally, 100 µL of the substrate solution containing 0.015 % (w/v) TMB was added and incubated at 37 °C for 30 min, followed by addition with 25 µL of 2 M H₂SO₄ and spectrometric determination at 450 nm.

2.14. Serum competition assay

The interaction between RBD and hACE2 was competitively inhibited by the mice serum. The competition assay was determined by surface plasmon resonance (SPR), using a Biacore S200 instrument (Cytiva Life Sciences, USA). RBD was biotinylated by the EZ-link-NHS-biotin reagent (Thermo Fisher Scientific). The biotinylated RBD (5 µg/mL) was injected over the Series S Sensor chip SA (Cytiva Life Sciences, USA) for 30 s at 10 µL/min. The sera of the RBD-IC28-M group on day 21 were harvested. An aliquot of serum from each mouse (5 µL) was mixed to obtain a mix representative of the RBD-IC28-M group. A two-fold dilution of the sera was loaded on the SA Sensor chip to saturate RBD for 300 s. Then, 400 nM hACE2 was associated with the chip for 300 s to detect the competitive binding signal. The chips were then regenerated with 10 mM glycine-HCl buffer (pH 2.5). Real-time signal data were collected, and the competition behavior was recorded.

2.15. Authentic SARS-CoV-2 virus neutralization assay

The neutralization assays with authentic SARS-CoV-2 virus were performed in a BSL-3 laboratory. In brief, the sera of the PBS, RBD and RBD-IC28-M groups were three-fold serially diluted starting at 1:30 by DMEM supplemented with 2 % FBS, 1 % penicillin and 1 % streptomycin, respectively. The diluted sera mixed with equal volumes of 100 tissue culture half-infective doses (TCID₅₀) of the SARS-CoV-2 strain (Wuhan-Hu-1, GenBank: NC 045512.2), followed by incubation at 37 °C for 2 h. Afterward, the mixture was added to Vero-E6 cells in 96-well plates and incubated for 96 h at 37 °C with 5 % CO₂. All diluted serum samples were tested in duplicate. The neutralization antibody titers of all the sera were defined as the reciprocal of serum dilution that could neutralize 50 % of the virus infection at 4 d postinfection.

2.16. Lymphocyte proliferation assay

The immunized BALB/c mice on day 21 were sacrificed. The spleens were aseptically removed. Fresh splenocytes were resuspended to 3 × 10⁵ cells/mL (96-well plates, 100 µL) in RPMI 1640 medium with 10 % (w/v) heat-inactivated FBS, 0.05 mM 2-mercaptoethanol, 100 IU/mL penicillin, and 100 µg/mL streptomycin for 36 h. The cells were subsequently stimulated with medium alone (negative control), 20 µg/mL RBD (experimental group) and 1 µg/mL ConA (positive control) for 24 h, respectively. Proliferation was assayed with CCK-8 vital stain (Dojindo Laboratories, USA). The stimulation index was calculated as the ratio of the average OD₄₅₀ value of the antigen-stimulated cells to that of the medium-stimulated cells. Experiments were performed in triplicate and repeated at least three times independently.

2.17. Cytokine secretion assay

Splenocytes of the immunized mice were diluted to 3 × 10⁵ cells/mL in RPMI-1640 medium containing 10 % FBS and 100 U/mL penicillin-streptomycin, followed by incubation with 20 µg/mL RBD for 68 h. The supernatant of splenocyte cultures was collected by centrifugation. The concentrations of IFN-γ, IL-5 and IL-10 in the supernatant were determined using the mouse cytokine ELISA kits, according to manufacturer's instructions. Experiments were performed in triplicate and repeated at least three times independently.

2.18. Toxicity study

The serum samples of the five groups on day 21 were collected for toxicity study. Creatine kinase (CK), lactate dehydrogenase (LDH), alanine aminotransferase (ALT), total protein (TP), albumin (ALB), and uric acid (UA) in the mice sera was determined, using an Analyzer Medical System (AUTO LAB, Italy). The levels of these substances were used to evaluate the potential toxicity of the conjugates to the cardiac, hepatic, and renal functions.

2.19. Statistical analysis

The differences between the experimental groups were compared by one-way ANOVA. Results were analyzed using GraphPad Prism 5 software (GraphPad Software, CA, USA). The values of P < 0.05 (*) and P < 0.01 (**) were considered statistically and highly statistically significant between the experimental groups, respectively.

3. Results

3.1. SEC analysis

The three conjugates were prepared by conjugation of RBD with IC28 and/or mannan. The three conjugates were purified from the reaction mixture by a semi-preparative Superdex 200 column. Afterwards, an analytical Sepharose 6 column (1.0 cm × 30 cm) was used to analyze the purified conjugates. As shown in Fig. 2a, RBD showed a single and symmetric elution peak at 20.4 mL. The single elution peak of RBD-IC28 (18.9 mL) was slightly left-shifted as compared with that of RBD. RBD-M was eluted as a wide peak at 16.6 mL that was left-shifted as compared with that of RBD-IC28. RBD-IC28-M exhibited a wide peak at 14.8 mL that was further left-shifted. No apparent by-product was observed during the chemical reaction. Thus, conjugation with IC28 and mannan synergistically enhanced the hydrodynamic volume of RBD.

3.2. SDS-PAGE analysis

As shown in Fig. 2b, RBD (Lane 2) exhibited a single electrophoresis band corresponding to an apparent Mw of ~27.0 kDa. As compared with RBD, RBD-IC28 (Lane 3) displayed a single band with a slower

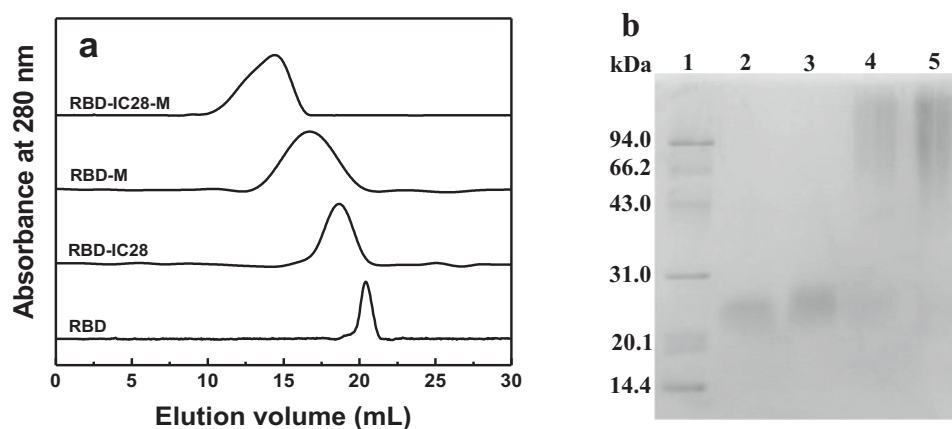


Fig. 2. Characterization of the three conjugates. The conjugates were analyzed by an analytical Sepharose 6 column (1 cm × 30 cm) at room temperature (a). The column was equilibrated and eluted by 20 mM PB buffer (pH 7.4) at a flow rate of 0.5 mL/min. The conjugates were analyzed by SDS-PAGE (b). Lane 1: marker; Lane 2: RBD; Lane 3: RBD-IC28; Lane 4: RBD-M; Lane 5: RBD-IC28-M.

migration, corresponding to an apparent Mw of ~30.0 kDa. This indicated that RBD was covalently conjugated with IC28. RBD-M (Lane 4) and RBD-IC28-M (Lane 5) both displayed a disperse electrophoresis band corresponding to an Mw of 60–150 kDa.

3.3. Quantitative assay

The RBD, IC28 and mannan contents of the conjugates were quantitatively analyzed. The mannan/IC28/RBD molar ratios of the conjugates were calculated by comparison of their contents. The mannan/

RBD molar ratios of RBD-M and RBD-IC28-M were 1.9 and 1.8, respectively. The IC28/RBD molar ratios of RBD-IC28 and RBD-IC28-M were 3.7 and 3.9, respectively. Thus, mannan, IC28 and RBD were at a comparable amount in the conjugates. Because RBD-IC28-M had an apparent Mw of 60–150 kDa, 2–5 RBD molecules (~27 kDa) were presumably conjugated with multiple IC28 (~1 kDa) and mannan (~3 kDa) in a lattice structure. Thus, the conjugate is not homogeneous in the molecular size.

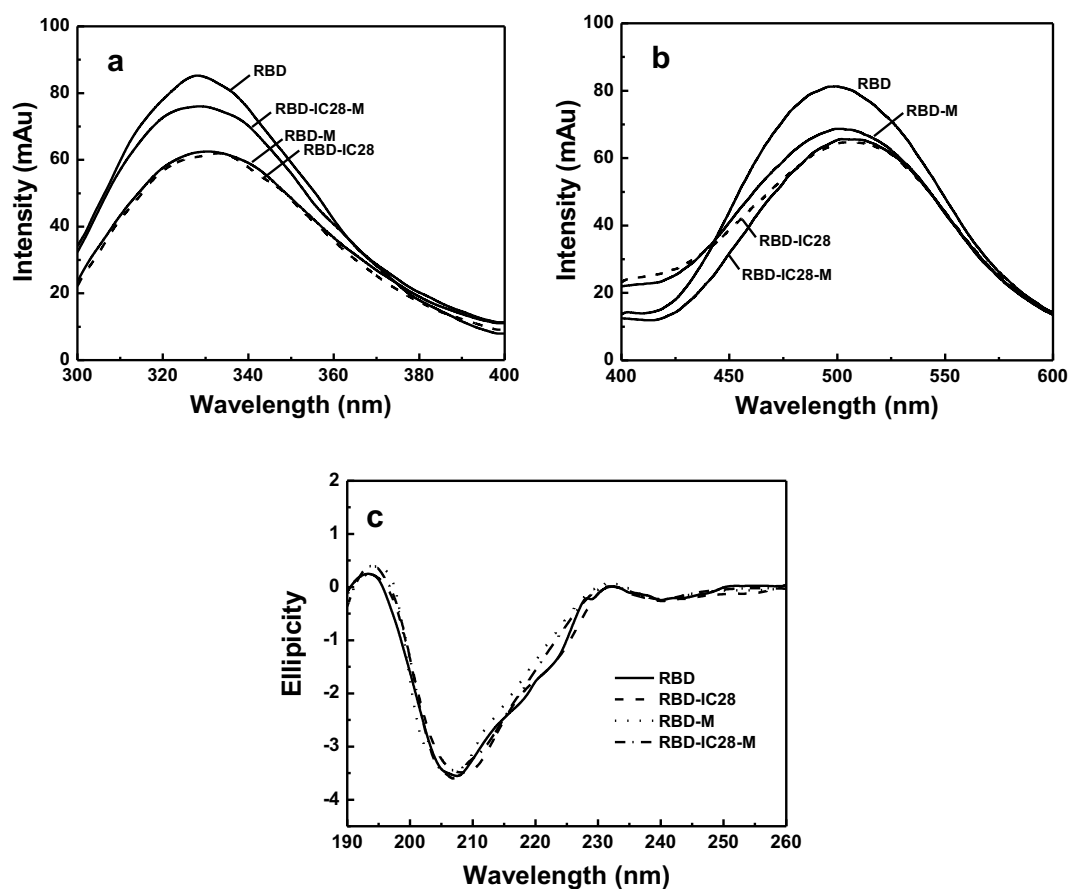


Fig. 3. Structural characterization of the three conjugates. The intrinsic fluorescence emission spectra (a) were recorded from 300 nm to 400 nm. The extrinsic fluorescence emission spectra (b) were recorded from 400 nm to 600 nm. The CD spectra (c) were recorded from 260 nm to 190 nm.

3.4. Fluorescence analysis

3.4.1. Intrinsic fluorescence spectroscopy

Intrinsic fluorescence was utilized to monitor the structural alteration of RBD upon conjugation with IC28 and mannan. As shown in Fig. 3a, the maximum emission fluorescence intensities of RBD were at 326 nm. As compared with RBD, RBD-IC28, RBD-M and RBD-IC28-M all displayed a slightly decrease in the fluorescence intensity with the maximum at 328 nm. This suggested that conjugation with IC28 and mannan slightly altered the tertiary structure of RBD.

3.4.2. Extrinsic fluorescence spectroscopy

The hydrophobicity of the three conjugates was measured by binding with a fluorescent probe, ANS. As shown in Fig. 3b, RBD showed an EF intensity with the maximum at 500 nm. The EF intensity of RBD-M was slightly higher than those of RBD-IC28 and RBD-IC28-M. As compared with RBD, RBD-IC28, RBD-M and RBD-IC28-M all displayed a slightly decrease in the EF intensity with the maximum at 503 nm. This suggested that covalent conjugation with IC28 and mannan increased the hydrophilicity of RBD and slightly decrease the EF intensity. Moreover, covalent conjugation increased the exposure of the hydrophobic residues of RBD to the surrounding environment, which rendered the occurrence of the obvious red shift.

3.5. Circular dichroism spectroscopy

Far-UV circular dichroism (CD) spectroscopy was utilized to determine the secondary structures of the three conjugates. As shown in Fig. 3c, the far-UV CD spectra of RBD displayed a positive peak at 198 nm and a negative maximum ellipticity around 208 nm, a characteristic of predominant β -sheet structure. Moreover, the CD spectra of RBD-

IC28, RBD-M and RBD-IC28-M were nearly identical to that of RBD. Particularly, the α -helix and β -sheet contents of RBD were 4.6 % and 74.7 %, respectively. The α -helix (4.4 %) and β -sheet contents (69.7 %) of RBD-IC28-M were comparable to those of RBD. Thus, the secondary structure of RBD was largely maintained upon conjugation with IC28 and mannan.

3.6. RBD-specific antibodies

3.6.1. RBD-specific IgG

The RBD-specific IgG titers of the mice sera were determined by ELISA assay. As shown in Fig. 4a, the RBD-specific IgG titers of the RBD group were 1.4×10^3 at the second dose (day 14) and 3.7×10^3 at the third dose (day 21), respectively. Similarly, the RBD-specific IgG titers of the three conjugates groups on day 21 were higher than those on day 14. The RBD-IC28, RBD-M and RBD-IC28-M groups on day 21 all exhibited higher RBD-specific IgG titers than the RBD group. In particular, the RBD-specific IgG titers of the RBD-IC28-M group (3.9×10^4) were higher than those of RBD-IC28 (1.4×10^4) and RBD-M groups (2.0×10^4). This reflected the synergistic adjuvant effects of conjugation with IC28 and mannan.

3.6.2. RBD-specific IgG subclasses

As shown in Fig. 4b and c, the three conjugates all elicited RBD-specific IgG1 and IgG2a titers. In particular, the Th2-type IgG1 titers (Fig. 4b) of the five groups were higher than the corresponding Th1-type RBD-specific IgG2a titers (Fig. 4c). This suggested a predominant Th2-type immune response and moderate Th1-type immune response. It should be mentioned that the RBD-IC28-M group showed the highest RBD-specific IgG1 (3.0×10^4) and IgG2a titers (6.5×10^3) among the five groups. This indicated that conjugation of IC28 and mannan

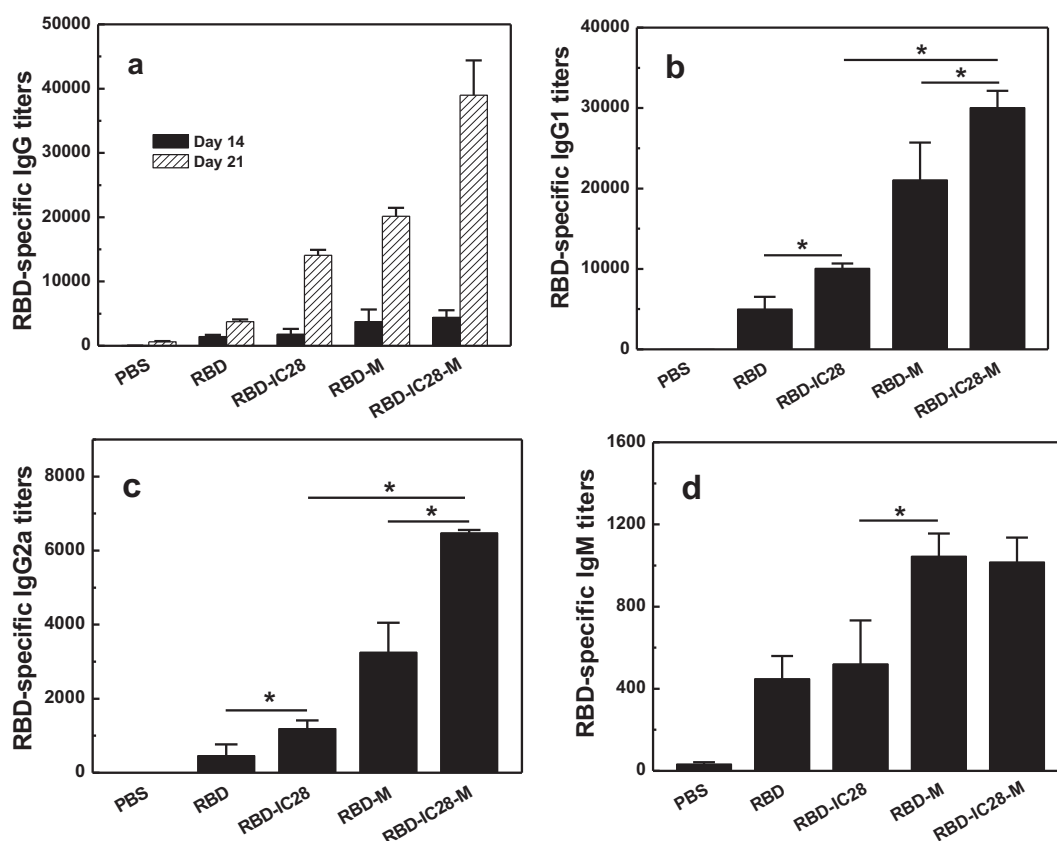


Fig. 4. RBD-specific antibody responses to the conjugates. The sera on days 14 and 21 were obtained for RBD-specific IgG measurement (a). The sera on day 21 were obtained for RBD-specific IgG1 (b), IgG2a (c) and IgM (d) measurements. Values represent the mean value \pm S.D. from 6 mice per group.

synergistically increased the Th1- and Th2-type immune response.

3.6.3. RBD-specific IgM

As shown in Fig. 4d, the RBD-specific IgM titers of the five groups were very low on day 21. As compared the RBD group at the third dose (4.5×10^2), the RBD-IC28, RBD-M and RBD-IC28-M groups showed 1.2-, 2.4- and 2.3-fold increases in the RBD-specific IgM titers on day 21. The RBD-specific IgM titers of the RBD-M group was comparable to those of the RBD-IC28-M group. This indicated that conjugation with IC28 and mannan increased the shift of the immune response from IgM to IgG.

3.7. Serum competition assay

The mice sera of the RBD-IC28-M group was subjected to a series of 2-fold dilution. The interaction between RBD and hACE2 in the presence of the diluted mice sera was evaluated by SPR. As shown in Fig. 5a, the several samples exhibited different response profiles during the incubation time of 300 s. After normalization of the initial response to zero, the response of the mixture in the presence of PBS buffer significantly increased as a function of incubation time (Fig. 5b), indicating the strong binding of RBD with hACE2. In contrast, the response of the mixture in the presence of the 8000-fold diluted serum was slightly lower than that in the presence of PBS buffer. The response of the mixture progressively decreased as the dilution fold decreased. This indicated that the serum could competitively inhibit the interaction between RBD and hACE2. In particular, the mixture in the presence of the 125- or 250-fold diluted sera was not responsive to the incubation time, indicating the 125- or 250-fold diluted sera could completely inhibit the interaction between RBD and hACE2.

3.8. Authentic SARS-CoV-2 virus neutralization assay

The neutralization ability of RBD-IC28-M against authentic SARS-CoV-2 virus was evaluated by the neutralization antibody titers of the immunized sera. As shown in Fig. 6a, the cell survival percentage of the three groups all decreased as the serum dilution increased in the presence of SARS-CoV-2. The cell survival percentage of the RBD-IC28-M group was higher than the RBD (64.3) and the PBS groups. This indicated that the neutralization antibody titer of the sera in the RBD-IC28-M group (201.4) was higher than that in the RBD (64.3) and the PBS groups (41.0). Thus, RBD-IC28-M exhibited a certain neutralization ability against authentic SARS-CoV-2 virus.

3.9. Antibody avidity

The antibody avidity reflected the bonding degree of RBD and the

RBD-specific IgG, and the induction of immunological memory. As indicated in Fig. 6b, the three conjugates all showed higher avidity index (AI) of the RBD-specific IgG than that of the RBD group (0.60). Particularly, the RBD-IC28-M group showed higher AI value (0.99) than the RBD-IC28 group (0.73) and the RBD-M group (0.95). This suggested that conjugation with IC28 and mannan synergistically increased the avidity of the RBD-specific IgG.

3.10. Antigenicity

The antigenicity of the three conjugates was characterized by detecting their binding affinity to hACE2, a critical characteristic enabling them to neutralize authentic SARS-CoV-2. As shown in Fig. 7, RBD exhibited higher binding affinity than RBD-IC28 as a function of hACE2 concentrations. It was due to that the conjugated IC28 partially shielded the binding domain of RBD with hACE2. In contrast, RBD-M and RBD-IC28-M both displayed a higher binding affinity than RBD as a function of hACE2 concentrations, which were comparable to each other.

3.11. RBD-specific splenocyte proliferation

Splenocyte proliferation can reflect the effectiveness of vaccine to induce the humoral and cellular immune response. Splenocyte proliferation index (PI) was measured after stimulation of splenocyte with the conjugates. As shown in Fig. 8a, the PI value of the RBD-IC28 group (2.2) was higher than that of the RBD group (1.7) ($P < 0.05$) and lower than that of the RBD-M group (2.6) ($P < 0.05$). Thus, conjugation with IC28 stimulated the RBD-specific splenocyte proliferation, and the ability was lower than conjugation with mannan. In particular, the PI value of the RBD-IC28-M group (2.8) was the highest in the five groups. This indicated that conjugation with IC28 and mannan synergistically increased the splenocyte proliferation.

3.12. Th1-type and Th2-type cytokines

The secretion pattern of cytokines was an important factor to direct the immune response. As a typical Th1-type cytokine, IFN- γ was responsible for macrophage activation. IL-5 and IL-10 were assayed as typical Th2-type cytokines. These cytokines in the cultures were measured by ELISA after stimulation with RBD.

As shown in Fig. 8, the PBS and the RBD groups both exhibited low levels of the three cytokines. As compared with the RBD group, the RBD-IC28 group showed 1.1-, 1.6-, and 1.6-fold increase in the IFN- γ (Fig. 8b), IL-5 (Fig. 8c) and IL-10 (Fig. 8d) levels, respectively. As compared with the RBD group, the RBD-M group showed 2.0-, 1.2- and

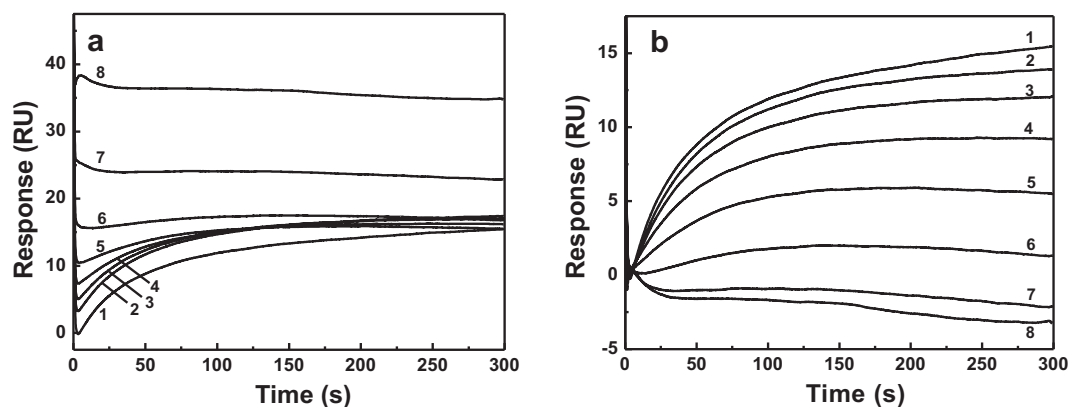


Fig. 5. SPR analysis of the interaction between RBD and hACE2 in the presence of the diluted mice sera. The responses before (a) and after normalization of the initial response to zero (b) were recorded during the incubation time of 300 s. The mixture of RBD and hACE2 was in the presence of PBS buffer (1), 8000- (2), 4000- (3), 2000- (4), 1000- (5), 500- (6), 250- (7), and 125-fold (8) diluted sera of the RBD-IC28-M group, respectively.

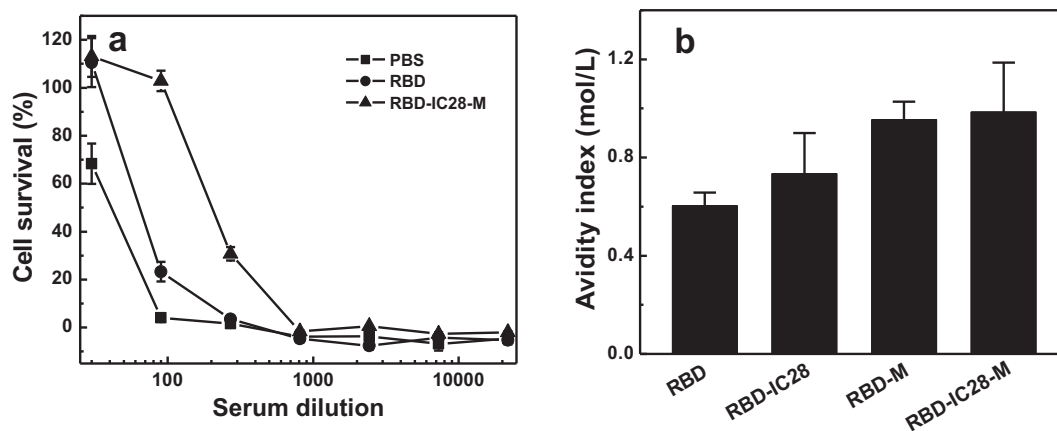


Fig. 6. Authentic virus neutralization assay and avidity analysis of RBD-specific IgG. The mouse sera on day 21 were used avidity analysis. Bar represents mean \pm S. D. from 6 mice per group.

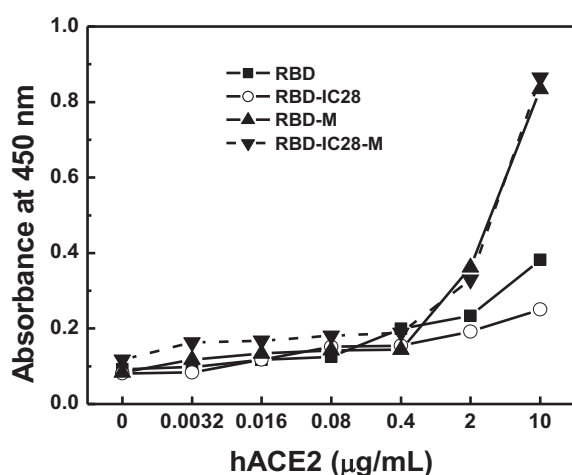


Fig. 7. The antigenicity of the conjugates.

2.0-fold increase in the IFN- γ , IL-5, and IL-10 levels, respectively. This suggested that conjugation with IC28 or mannan could increase the Th1- and Th2-type immune responses to RBD. In particular, the RBD-IC28-M group showed the highest cytokine levels in the five groups. As compared with the RBD group, the RBD-IC28-M group showed 2.9-, 1.8- and 2.4-fold increase in the IFN- γ , IL-5 and IL-10 levels, respectively. Thus, conjugation of IC28 and mannan showed the additive effect to increase the Th1- and Th2-type immune responses to RBD.

3.13. Toxicity study

Because antibody-drug conjugates (ADC) may render clinical toxicity [48], it was necessary to evaluate the potential toxicity of RBD-IC28-M. CK and LDH indicated the cardiac function; ALT, TP and ALB reflected the hepatic function; UA revealed the renal function. The levels of these substances in the sera were determined to evaluate their potential toxicity to the cardiac, hepatic and renal functions of mice.

As shown in Table 1, the PBS group showed certain levels of these substances. As compared with the PBS group, the RBD group showed no significant differences in these parameters except a slightly higher LDH level. The RBD-M group showed no significant differences in these parameters except slightly lower LDH and CK levels. The RBD-IC28-M group showed no significant differences in these parameters except a slightly lower CK level. This indicated that the three conjugates showed no apparent toxicity to the cardiac, hepatic and renal functions of mice.

4. Discussion

At present, it is necessary to develop affordable and accessible SARS-CoV-2 vaccines that can provide immune protection especially for low- and middle-income countries. RBD expressed by *E. coli* is amenable to low cost and high-yield manufacturability with the general expression yield of 0.1–2 g/L. In the present study, RBD from *E. coli*, IC28 and mannan were conjugated in one entity (RBD-IC28-M). As two TLR ligands, IC28 and mannan both acted as the adjuvants for RBD. A SARS-CoV-2 vaccine formulated by covalent conjugation of RBD with IC28 and mannan represented a promising strategy to address this need. The immunogenicity, antigenicity, viral neutralization and preliminary safety of RBD-IC28-M were evaluated.

After in vitro stimulation with RBD, the splenocytes of the RBD-IC28-M group generate high levels of IFN- γ (75.1 ng/mL), a Th1-type cytokine related to the innate immunity essential to control the viral infection. RBD-IC28-M promoted high secretion levels of IL-5 (2675.5 pg/mL) and IL-10 (688.1 pg/mL), two Th2-type cytokines in BALB/c mice. RBD-IC28-M could strongly stimulate the splenocyte proliferation with a PI value of 2.2. Thus, a potent cellular immune response was stimulated by RBD-IC28-M. RBD-IC28-M also elicited high RBD-specific IgG titers (3.9×10^4). Thus, RBD-IC28-M elicited a strong humoral immune response. Moreover, the IgG2a and IgG1 levels increased after three immunizations, indicating that booster immunizations led to memory B-cell activation.

After being infected by SARS-CoV-2, the viral infection may be restrained by the rapidly-induced specific neutralizing antibodies (NABs). The SARS-CoV-2 S protein is the primary target of NABs, and the immunodominant RBD accounts for >90 % of the neutralizing activity in the COVID-19 convalescent sera and vaccinated individuals. As the antigen of RBD-IC28-M, RBD from *E. coli* could bind ACE2 with a K_D of 2.98×10^{-8} M, which was 7.0-fold of K_D of RBD expressed by the HEK293 cells [48]. This was due to the absence of the disulfide bond formation and glycosylation in RBD from *E. coli*. In our study, RBD-IC28-M elicited a NAb titer of 201.4 in the BALB/c mice, indicating a certain neutralizing activity against SARS-CoV-2. In addition, the cellular immunity elicited by RBD-IC28-M was expected to clear SARS-CoV-2. Next study should be focused on the cellular immunity of RBD-IC28-M.

Conjugation of IC28 and mannan did not apparently alter the structure of RBD. Mannan, a ligand of TLR-4 or TLR-2, could be recognized via mannose receptor, dectin-2, and DC-SIGN, which induce Th1-type and Th2-type immune response. Flagellin is a microbe-associated molecular pattern that strongly activates the innate and adaptive immune systems [42]. However, its intrinsic antigenicity may be an obstacle for clinical development, since the generation of flagellin-specific antibodies can preclude the presence of adjuvant activity

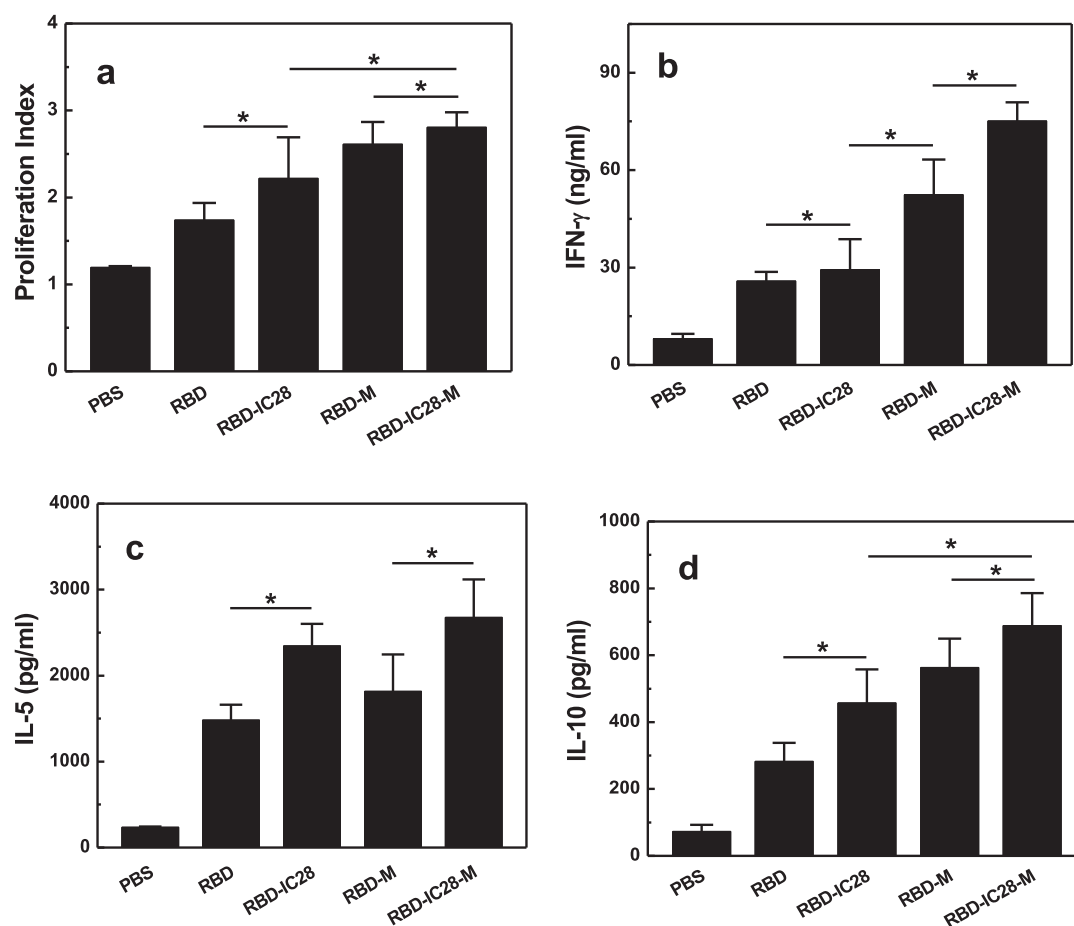


Fig. 8. Determination of splenocyte proliferation index and the cytokine secretions in the immunized BALB/c mice. Splenocyte proliferation index (a) was measured at 450 nm by CCK8. IFN- γ (b), IL-5 (c) and IL-10 (d) were analyzed using the ELISA kits. Values represented the mean value \pm S.D. from 6 mice per group.

Table 1

Toxicity study on the cardiac, hepatic and renal functions of the mice.

Sample	LDH ^a (U/L)	CK ^b (U/L)	ALT ^c (U/L)	ALB ^d (g/L)	TP ^e (g/L)	UA ^f (μ mol/L)
PBS	707.0	757.2	34.8	34.2	63.2	127.0
RBD	901.2	658.4	39.6	33.6	53.6	159.6
RBD-IC28	667.8	502.0	29.4	33.4	55.0	142.2
RBD-M	483.0	505.8	29.8	33.0	58.8	148.0
RBD-IC28-M	613.0	382.6	29.2	33.2	59.4	114.4

^a Lactate dehydrogenase.

^b Creatine kinase.

^c Alanine aminotransferase.

^d Albumin.

^e Total protein.

^f Uric acid.

[42]. Interestingly, IC28 from bacterial flagellin stimulated the TLR5 but displayed very low intrinsic antigenicity [41]. In our study, RBD-IC28-M elicited significantly stronger immune responses than the RBD conjugated with IC28 or mannan alone (RBD-IC28 and RBD-M). Thus, IC28 and mannan could play the immunomodulatory activities for RBD in an additive manner.

In RBD-IC28-M, 2–5 RBD molecules were conjugated with multiple IC28 and mannan molecules in a lattice structure. This could increase the epitopes of RBD and the avidities between RBD and B cell receptors through the polyvalency effect. Conjugation ensured that RBD, IC28 and mannan simultaneously reached the APCs. In addition, multimerization of RBD in RBD-IC28-M increased the antigenicity of the epitopes and

enhanced its hACE2-binding affinity, which in turn increased the immunogenicity relative to soluble antigen. As a multi-epitopic vaccine, RBD-IC28-M could thus provide immunological diversity of response. Moreover, the side effect of RBD expressed by *E. coli* was similar to that of RBD expressed by HEK293 that was used for the current SARS-CoV-2 vaccines.

5. Conclusion

The conjugate (RBD-IC28-M) could elicit potent RBD-specific humoral and cellular immune responses. RBD-IC28-M elicited high RBD-specific IgG titers, and a neutralization antibody titer of 201.4. It also induced high levels of Th1-type cytokines (IFN- γ) and Th2-type cytokines (IL-5 and IL-10), along with high antigenicity and no apparent toxicity to the organs. The sera of the RBD-IC28-M group could competitively interfere with the interaction of RBD and ACE2. In addition, conjugation of IC28 and mannan with RBD showed an additive immunoproliferative effect to increase the humoral and cellular immune response to RBD. Thus, conjugation of RBD with IC28 and mannan may represent a promising approach to enhance the immunogenicity of RBD against SARS-CoV-2. Moreover, our conjugation strategy may provide a platform for preparation of protein-based vaccines against the emerging viruses, such as monkey pox virus.

CRediT authorship contribution statement

This manuscript has not been published or submitted for publication. All authors have seen and approved the submission of the manuscript.

Declaration of competing interest

The authors declare that they have no known competing financial interests or personal relationships that could have appeared to influence the work reported in this paper.

Acknowledgements

This study was financially supported by Beijing Natural Science Foundation (M21013), National Natural Science Foundation of China (82271869 and 31970875), and National Key Research and Development Project of China (2018YFA0900804).

References

- [1] P. V'kovski, A. Kratzel, S. Steiner, H. Stalder, V. Thiel, Coronavirus biology and replication: implications for SARS-CoV-2, *Nat. Rev. Microbiol.* 19 (2021) 155–170.
- [2] B. Hu, H. Guo, P. Zhou, Z.L. Shi, Characteristics of SARS-CoV-2 and COVID-19, *Nat. Rev. Microbiol.* 19 (2021) 141–154.
- [3] S. Nawaz, COVID-19, SARS-CoV-2, origin, transmission and treatment aspects, a brief review, *Infect. Disord. Drug Targets* 21 (2021), e270421186673.
- [4] WHO, Novel Coronavirus 2019 (2022), Available at, <https://www.who.int/emergencies/diseases/novel-coronavirus-2019>.
- [5] K. Kupferschmidt, Where did 'weird' omicron come from? *Science* 374 (6572) (2021) 1179.
- [6] J.A. Al-Tawfiq, V.T. Hoang, N. Le Bui, D.T. Chu, Z.A. Memish, The emergence of the omicron (B.1.1.529) SARS-CoV-2 variant: what is the impact on the continued pandemic? *J. Epidemiol. Glob. Health* 12 (2022) 143–146.
- [7] D.T. Chu, S.M. Vu Ngoc, H. Vu Thi, Y.V. Nguyen Thi, T.T. Ho, et al., COVID-19 in southeast Asia: current status and perspectives, *Bioengineered* 13 (2022) 3797–3809.
- [8] H. Jhun, H.Y. Park, Y. Hisham, C.S. Song, S. Kim, SARS-CoV-2 delta (B.1.617.2) variant: a unique T478K mutation in receptor binding motif (RBM) of spike gene, *Immune Netw.* 21 (2021), e32.
- [9] V. Izda, M.A. Jeffries, A.H. Sawalha, COVID-19: a review of therapeutic strategies and vaccine candidates, *Clin. Immunol.* 222 (2021), 108634.
- [10] O. Sharma, A.A. Sultan, H. Ding, C.R. Triggie, A review of the progress and challenges of developing a vaccine for COVID-19, *Front. Immunol.* 11 (2021), 585354.
- [11] H. Wang, Y. Zhang, B. Huang, W. Deng, Y. Quan, W. Wang, et al., Development of an inactivated vaccine candidate, BBIBP-CorV, with potent protection against SARS-CoV-2, *Cell* 182 (2020) 713–721.
- [12] F.C. Zhu, X.H. Guan, Y.H. Li, J.Y. Huang, T. Jiang, L.H. Hou, et al., Immunogenicity and safety of a recombinant adenovirus type-5-vectored COVID-19 vaccine in healthy adults aged 18 years or older: a randomised, double-blind, placebo-controlled, phase 2 trial, *Lancet* 396 (2020) 479–488.
- [13] L. Feng, Q. Wang, C. Shan, C. Yang, Y. Feng, J. Wu, et al., An adenovirus-vectored COVID-19 vaccine confers protection from SARS-COV-2 challenge in rhesus macaques, *Nat. Commun.* 11 (2020) 4207.
- [14] J. Yu, L.H. Tostanoski, L. Peter, N.B. Mercado, K. McMahan, S.H. Mahrokhian, et al., DNA vaccine protection against SARS-CoV-2 in rhesus macaques, *Science* 369 (2020) 806–811.
- [15] F.P. Polack, S.J. Thomas, N. Kitchin, J. Absalon, A. Gurtman, S. Lockhart, et al., Safety and efficacy of the BNT162b2 mRNA COVID-19 vaccine, *N. Engl. J. Med.* 383 (2020) 2603–2615.
- [16] W.C. Huang, S. Zhou, X. He, K. Chiem, M.T. Mabrouk, et al., SARS-CoV-2 RBD neutralizing antibody induction is enhanced by particulate vaccination, *Adv. Mater.* 32 (2020), e2005637.
- [17] S. Xia, Y. Zhang, Y. Wang, H. Wang, Y. Yang, G.F. Gao, et al., Safety and immunogenicity of an inactivated SARS-CoV-2 vaccine, BBIBP-CorV: a randomised, double-blind, placebo-controlled, phase 1/2 trial, *Lancet Infect. Dis.* 21 (2021) 39–51.
- [18] C. Keech, G. Albert, I. Cho, A. Robertson, P. Reed, S. Neal, et al., Phase 1–2 trial of a SARS-CoV-2 recombinant spike protein nanoparticle vaccine, *N. Engl. J. Med.* 383 (2020) 2320–2332.
- [19] S. Chenchula, P. Karunakaran, S. Sharma, M. Chavan, Current evidence on efficacy of COVID-19 booster dose vaccination against the omicron variant: a systematic review, *J. Med. Virol.* 94 (2022) 2969–2976.
- [20] T. Fiolet, Y. Kherabi, C.J. MacDonald, J. Ghosn, N. Peiffer-Smadja, Comparing COVID-19 vaccines for their characteristics, efficacy and effectiveness against SARS-CoV-2 and variants of concern: a narrative review, *Clin. Microbiol. Infect.* 28 (2022) 202–221.
- [21] W.C. Koff, T. Schenkelberg, T. Williams, R.S. Baric, A. McDermott, C.M. Cameron, et al., Development and deployment of COVID-19 vaccines for those most vulnerable, *Sci. Transl. Med.* 13 (2021) eabd1525.
- [22] O. Sharma, A.A. Sultan, H. Ding, C.R. Triggie, A review of the progress and challenges of developing a vaccine for COVID-19, *Front. Immunol.* 11 (2020), 585354.
- [23] P.T. Heath, E.P. Galiza, D.N. Baxter, M. Boffito, D. Browne, et al., Safety and efficacy of NVX-CoV2373 COVID-19 vaccine, *N. Engl. J. Med.* 385 (2021) 1172–1183.
- [24] S.B. Kadam, G.S. Sukhramani, P. Bishnoi, A.A. Pable, V.T. Barvkar, SARS-CoV-2, the pandemic coronavirus: molecular and structural insights, *J. Basic Microbiol.* 61 (2021) 180–202.
- [25] R. Arya, S. Kumari, B. Pandey, H. Mistry, S.C. Bihani, A. Das, et al., Structural insights into SARS-CoV-2 proteins, *J. Mol. Biol.* 433 (2021), 166725.
- [26] J. Yang, W. Wang, Z. Chen, S. Lu, F. Yang, Z. Bi, et al., A vaccine targeting the RBD of the S protein of SARS-CoV-2 induces protective immunity, *Nature* 586 (2020) 572–577.
- [27] F. Chiuppesi, M.D. Salazar, H. Contreras, V.H. Nguyen, J. Martinez, Y. Park, et al., Development of a multi-antigenic SARS-CoV-2 vaccine candidate using a synthetic poxvirus platform, *Nat. Commun.* 11 (2020) 6121.
- [28] H. Kleanthous, J.M. Silverman, K.W. Makar, I.K. Yoon, N. Jackson, D.W. Vaughn, Scientific rationale for developing potent RBD-based vaccines targeting COVID-19, *NPJ Vaccines* 6 (2021) 128.
- [29] C.R. Arbeitman, G. Auge, M. Blaustein, L. Bredeston, E.S. Corapi, P.O. Craig, et al., Structural and functional comparison of SARS-CoV-2 spike receptor binding domain produced in *Pichia pastoris* and mammalian cells, *Sci. Rep.* 10 (2020) 21779.
- [30] W. Tai, L. He, X. Zhang, J. Pu, D. Voronin, S. Jiang, Y. Zhou, L. Du, Characterization of the receptor-binding domain (RBD) of 2019 novel coronavirus: implication for development of RBD protein as a viral attachment inhibitor and vaccine, *Cell Mol. Immunol.* 17 (2020) 613–620.
- [31] W.H. Chen, P.J. Hotez, M.E. Bottazzi, Potential for developing a SARS-CoV receptor-binding domain (RBD) recombinant protein as a heterologous human vaccine against coronavirus infectious disease (COVID)-19, *Hum. Vaccin. Immunother.* 16 (2020) 1239–1242.
- [32] A.R. Marquez-Ipina, E. Gonzalez-Gonzalez, I.P. Rodriguez-Sanchez, I.M. Lara-Mayorga, L.A. Mejía-Manzano, M.G. Sánchez-Salazar, et al., Serological test to determine exposure to SARS-CoV-2: ELISA based on the receptor-binding domain of the spike protein (S-RBD (N318–V510)) expressed in *Escherichia coli*, *Diagnostics* 11 (2021) 271.
- [33] Y. He, J. Qi, L. Xiao, L. Shen, W. Yu, T. Hu, Purification and characterization of the receptor-binding domain of SARS-CoV-2 spike protein from *Escherichia coli*, *Eng. Life Sci.* 21 (2021) 453–460.
- [34] M.L. Bellone, A. Puglisi, F.D. Piaz, A. Hochkoeppler, Production in *Escherichia coli* of recombinant COVID-19 spike protein fragments fused to CRM197, *Biochem. Biophys. Res. Commun.* 558 (2021) 79–85.
- [35] S. Yang, Y. Li, L. Dai, J. Wang, P. He, C. Li, et al., Safety and immunogenicity of a recombinant tandem-repeat dimeric RBD-based protein subunit vaccine (ZF2001) against COVID-19 in adults: two randomised, double-blind, placebo-controlled, phase 1 and 2 trials, *Lancet Infect. Dis.* 21 (2021) 1107–1119.
- [36] K.S. Park, X. Sun, M.E. Aikins, J.J. Moon, Non-viral COVID-19 vaccine delivery systems, *Adv. Drug Deliv. Rev.* 169 (2021) 137–151.
- [37] T.J. Moyer, A.C. Zmolek, D.J. Irvine, Beyond antigens and adjuvants: formulating future vaccines, *J. Clin. Invest.* 126 (2016) 799–808.
- [38] C. Exley, An aluminium adjuvant in a vaccine is an acute exposure to aluminium, *J. Trace Elem. Med. Biol.* 57 (2020) 57–59.
- [39] N. Garcon, P. Chomez, M. Van Mechelen, GlaxoSmithKline adjuvant systems in vaccines: concepts, achievements and perspectives, *Expert Rev. Vaccines* 6 (2007) 723–739.
- [40] I.A. Hajam, P.A. Dar, I. Shah Nawaz, J.C. Jaume, J.H. Lee, Bacterial flagellin—a potent immunomodulatory agent, *Exp. Mol. Med.* 49 (2017), e373.
- [41] M.E. Biedma, D. Cayet, J. Tabareau, A.H. Rossi, K. Ivicak-Kocjan, G. Moreno, et al., Recombinant flagellins with deletions in domains D1, D2, and D3: characterization as novel immunoadjuvants, *Vaccine* 37 (2019) 652–663.
- [42] C. Nempont, D. Cayet, M. Rumbo, C. Bompard, V. Villeret, J.C. Sirard, Deletion of flagellin's hypervariable region abrogates antibody-mediated neutralization and systemic activation of TLR5-dependent immunity, *J. Immunol.* 181 (2008) 2036–2043.
- [43] H.Y. Son, V. Apostolopoulos, C.W. Kim, Mannosylated T/Tn with Freund's adjuvant induces cellular immunity, *Int. J. Immunopathol. Pharmacol.* 31 (2018), 394632017742504.
- [44] J. Qi, Y. He, L. Shen, W. Yu, T. Hu, Conjugation of hemoglobin and mannan markedly improves the immunogenicity of domain III of the Zika virus E protein: structural and immunological study, *Bioconjug. Chem.* 32 (2021) 328–338.
- [45] Y. He, W. Yu, L. Xiao, L. Shen, J. Qi, T. Hu, Conjugation of Zika virus EDIII with CRM197, 8-arm PEG and mannan for development of an effective Zika virus vaccine, *Int. J. Biol. Macromol.* 190 (2021) 713–721.
- [46] Q. Huang, W. Yu, T. Hu, A potent antigen-adjuvant delivery system by conjugation of mycobacterium tuberculosis Ag85B-HspX fusion protein with arabinogalactan-poly(I:C) conjugate, *Bioconjug. Chem.* 27 (2016) 1165–1174.
- [47] I.A. Silverira, R.C. Bastos, M.S. Neto, A.P. Laranjeira, E.F. Assis, et al., Characterization and immunogenicity of meningococcal group C conjugate vaccine prepared using hydrazide-activated tetanus toxoid, *Vaccine* 25 (2007) 7261–7270.
- [48] J.C. Masters, D.J. Nickens, D. Xuan, R.L. Shazer, M. Amantea, Clinical toxicity of antibody drug conjugates: a meta-analysis of payloads, *Investig. New Drugs* 36 (2018) 121–135.